Film Thickness Dependence of the Surface Structure of Immiscible Polystyrene/Poly(methyl methacrylate) Blends

Keiji Tanaka, Atsushi Takahara, and Tisato Kajiyama*

Department of Chemical Science & Technology, Faculty of Engineering, Kyushu University, 6-10-1 Hakozaki, Higashi-ku, Fukuoka 812-81, Japan

Received August 7, 1995; Revised Manuscript Received December 20, 1995[⊗]

ABSTRACT: The film thickness dependence of surface structure for immiscible polystyrene/poly(methyl methacrylate) (PS/PMMA) films was investigated on the basis of atomic force microscopic observation and X-ray photoelectron spectroscopic measurement. In the case of the PS/PMMA film of 25 μm thickness, the air−polymer interfacial region was covered with a PS rich overlayer due to its lower surface free energy compared with that of PMMA and a well-defined macroscopic phase-separated structure was formed in the bulk phase. Also, in the case of the PS/PMMA thin film of 100 nm thickness, the phase-separated structure, in which the PMMA rich domains separated out of the PS rich matrix, formed at the film surface. The formation of the surface structure for the PS/PMMA thin film can be attributed to either the chain conformation or chain aggregation structure being frozen at the air−polymer interfacial region before the formation of a PS rich overlayer due to the fairly fast evaporation of solvent molecules. On the other hand, the two-dimensional PS/PMMA ultrathin film of 10.2 nm thickness did not show distinct phase-separated structure. When the film thickness became thinner than 10.2 nm, the two-dimensional PS/PMMA ultrathin film of 6.7 nm thickness showed fine and distinct phase-separated structure with the domain size of a few hundred nanometers. This structure can be designated as "mesoscopic phase-separated structure". The surface phase state for the two-dimensional PS/PMMA ultrathin films can be explained by the film thickness dependence of both the interaction parameter and the degree of entanglement among polymer chains.

Introduction

Investigations of surface structure for multicomponent polymer systems have been extensively done for the last decade, both experimentally[1−8] and theoretically,[9] with respect to associated functional properties such as blood compatibility, lubricant, wetting, permeability, and so on. It has been revealed that the surface structure of multicomponent polymer systems is fairly different from that in the bulk, that is, a lower surface free energy component is generally enriched in the surface region in order to minimize the air−polymer interfacial free energy. Also, for the past few years, surface molecular motions of polymeric solids have been paid great attention by several groups[10−16] due to their importance in practical applications. Both vigorous thermal molecular motion and thermal instability of polymeric chains at the surface can be explained by the larger free volume fraction at the surface region compared with that in the bulk due to the preferential segregation of chain end groups at the surface region[11,13,14] and/or the unsymmetrical environment at the air−polymer interface.[13,14]

Polymeric films of whose thicknesses are less than about twice the radius of gyration of an unperturbed chain, $2R_g$, can be defined as two-dimensional ultrathin films.[17−19] Then, the polymeric blend films with thicknesses less than $2R_g$ of the higher molecular weight component can be defined as the two-dimensional ultrathin blend films.[20] A flexible polymer chain in an ultrathin film is in a nonequilibrium state, since the conformational entropy of an individual chain in a constrained thin region is reduced in comparison with that in a three-dimensional solid state.[19] Since polymeric chains at the interface, in general, are thermally unstable, the molecular aggregation structure in the two-dimensional ultrathin film of binary polymer blend must be greatly different from that in the thick film. The authors have investigated the film thickness dependence of surface structure for the miscible polystyrene/poly(vinyl methyl ether) (PS/PVME) blend films.[20] Even though the blend system was miscible in the bulk region, it was revealed that surface phase-separated structure was formed even at the temperature below the bulk phase separation temperature in the case of the two-dimensional ultrathin state. The mechanism of surface phase separation for the PS/PVME ultrathin film could be explained by two factors: the negative spreading coefficient of PVME on the PS matrix and the remarkably reduced conformational entropy of a PVME chain due to stretching.

Internal phase-separated morphology for immiscible polymer blend films has been studied by several groups.[21−23] Shiraga et al. investigated the bulk phase-separated structure of the immiscible PS/poly(methyl methacrylate) (PS/PMMA) blend film on the basis of field-emission scanning electron microscopic observation.[21] They revealed that macroscopic phase-separated domains with a few micrometers in diameter were formed in the bulk region of the thick film. Winnik and co-workers investigated the depth profiling of the phase-separated structure for the PS/PMMA blend film on the basis of laser confocal fluorescence microscopic observation.[23] They revealed that the mechanism of phase separation at the film surface was fairly different from that in a bulk phase. However, it is still questionable and interesting which macroscopic phase-separated structure is formed in the constrained narrow space of the two-dimensional immiscible blend ultrathin film. The purpose of this study is to reveal the film thickness dependence of surface phase-separated structure of the immiscible PS/PMMA blend films.

* To whom correspondence should be addressed TEL: +81-92-641-1101 (ext. 5601). FAX: +81-92-651-5606.

[⊗] Abstract published in *Advance ACS Abstracts,* February 15, 1996.

0024-9297/96/2229-3232$12.00/0

Table 1. Characterizations of PS and PMMA Used in This Study

	M_n	M_w/M_n	$2R_g$/nm	γ/mJ·m^{-2}	T_g/K
PS	90k	1.05	16.6	40.2	378.2
PMMA	69k	1.06	14.6	41.2	403.2

Experimental Section

Materials. Polymers used in this study were monodisperse PS and PMMA. PS was synthesized by a living anionic polymerization method at 293 K using *sec*-butyllithium as an initiator. PMMA was also made in tetrahydrofuran by a living anionic polymerization at 196 K using *n*-butyllithium-added 1,1-diphenylethylene as an initiator. Table 1 shows characterizations of PS and PMMA. A number-average molecular weight, M_n, and a molecular weight distribution, M_w/M_n, were determined via gel permeation chromatography with polystyrene standards. The radius of gyration of an unperturbed chain was calculated by

$$R_g = (Nb^2/6)^{1/2} \quad (1)$$

where N is the degree of polymerization and b is the average statistical segment length. The magnitudes of b_{PS} and b_{PMMA} are 0.68 and 0.69 nm, respectively.[24] The surface free energy, γ, was determined by static contact angle measurement on the basis of Owens' procedure.[25]

Film Preparation. A PS/PMMA blend solution was prepared by mixing each in the toluene solution. The PS/PMMA blend ratio was designated as (weight %/weight %). The PS/PMMA blend thin and ultrathin films were prepared by a spin-coating method at 293 K. Film thickness was controlled by the concentration of the solution and the spin rates. Also, the blend thick films were prepared by a conventional solvent cast method. The film thickness of the thin or the ultrathin films was evaluated as follows. After a crater was formed in the polymer film by an ion beam sputtering or a cantilever tip scratch, its average step height, corresponding to the film thickness, was measured by atomic force microscopic (AFM) and/or scanning electron microscopic observations. The substrates used in this study are three types, that is, gold, silicon wafer, and siliconized cover glass, which have different degrees of interaction with PS or PMMA segments. The gold substrate does not fairly interact with PS and PMMA segments. A gold surface was coated on a silicon wafer by a sputter-coating method. It was impossible to measure the exact water contact angle for the gold substrate due to its instability in air. The cleaned silicon wafer was used as the hydrophilic surface. The silicon wafer was heated at 773 K for 3 h in order to remove residual organics on the surface and then was placed into a mixed solution of concentrated H_2SO_4 and 30% H_2O_2 (70/30 v/v) at 393 K for 1 h. The water contact angle of the cleaned Si wafer was 0°. The siliconized cover glass was used as the hydrophobic surface. Its static water contact angle was 88.7°. Although it was impossible to evaluate quantitatively the magnitudes of surface free energy for all these substrates, it was reasonable that the order of the magnitude of surface free energy was qualititatively in the order silicon > gold > siliconized substrate.

Surface Characterization. The surface morphology of the PS/PMMA blend films was investigated on the basis of AFM observation. The AFM images were obtained by SPA 300 with an SPI 3700 controller (Seiko Instruments Industry Co., Ltd.) at room temperature. The AFM cantilever used was microfabricated from Si_3N_4, and its spring constant was 0.022 N·m^{-1}. AFM observation was carried out in a repulsive force range of ca. 1 nN. The surface chemical composition of the PS/PMMA thin film was evaluated on the basis of X-ray photoelectron spectroscopic (XPS) measurement. The XPS spectra were obtained with an ESCA 850 (Shimadzu Co., Ltd.) at room temperature. The XPS measurement was performed under conventional conditions with a Mg Kα source at 8 kV and 30 mA. The emission angle of the photoelectron was 90°. The main chamber of the XPS instrument was maintained at ~10^{-6} Pa. All C_{1s} peaks were calibrated to a binding energy of 285.0 eV for neutral carbon, in order to correct these charging energy shifts.

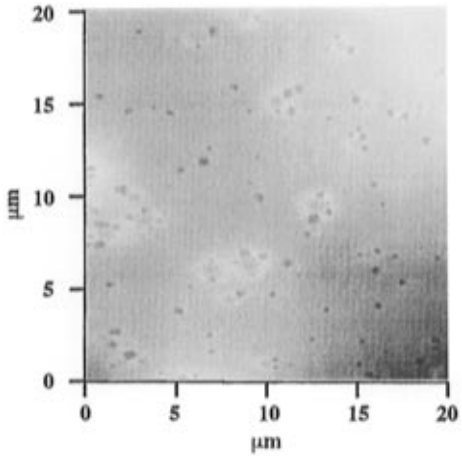

Figure 1. Atomic force microscopic image of the polystyrene/poly(methyl methacrylate) (30/70) thick film of 25 μm thickness coated on the gold substrate.

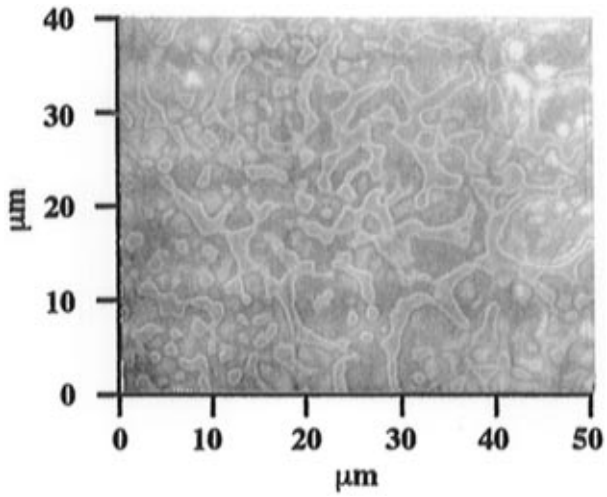

Figure 2. Phase contrast microscopic image for the PS/PMMA (30/70) thick film of 25 μm thickness coated on the gold substrate.

Results and Discussion

Thick Films of 25 μm Thickness. The phase-separated structure for the PS/PMMA film of 25 μm thickness was investigated in order to compare with those of the thin and the ultrathin films. Figures 1 and 2 show the AFM and the phase contrast microscopic (PCM) images of the PS/PMMA (30/70) film of 25 μm thickness coated on the gold substrate, respectively. The thick film was coated by a standard solvent-casting method at 293 K. AFM and PCM observations revealed that, although the surface was not in an apparent phase-separated state as shown in Figure 1, well-defined sea-island-like macroscopic phase-separated structure was formed in the bulk phase, as shown in Figure 2. Also, XPS measurement revealed that the PMMA weight fraction at the air−polymer interface was 8.4%, which was strikingly lower than that of the bulk composition, and in other words, PS segments were enriched at the film surface due to its lower surface free energy compared with that of PMMA even though the phase-separated structure was observed in the bulk phase. Thus, in the case of the PS/PMMA thick film, it seems reasonable to conclude that a PS rich overlayer is formed at the air−polymer interface and macroscopic

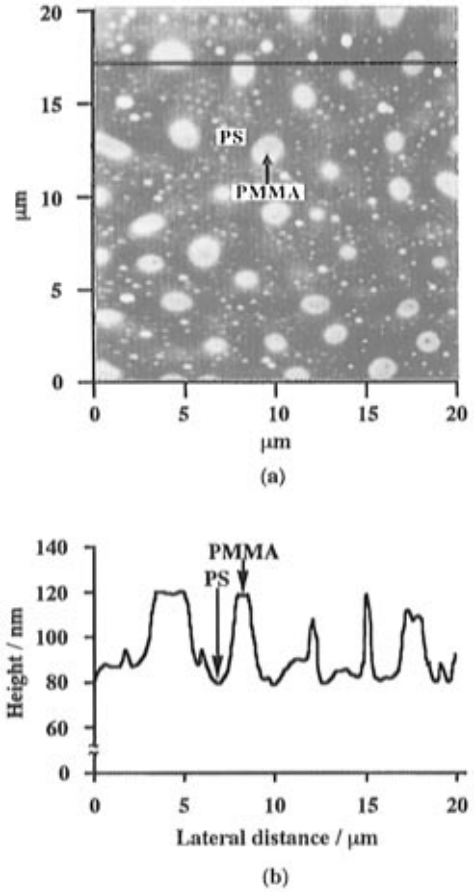

Figure 3. (a) AFM image and (b) sectional view along the line in the AFM image for the PS/PMMA (50/50) thin film of 100 nm thickness coated on the gold substrate.

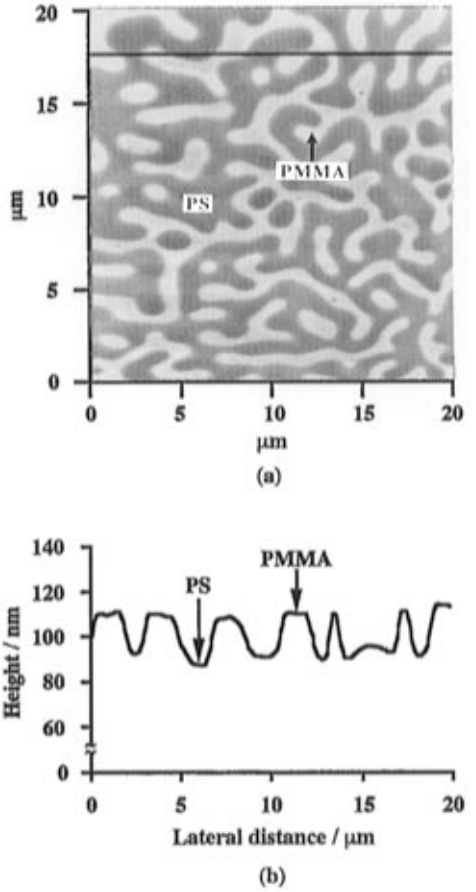

Figure 4. (a) AFM image and (b) sectional view along the line in the AFM image for the PS/PMMA (30/70) thin film of 100 nm thickness coated on the gold substrate.

phase-separated structure is formed in a bulk phase. The surface structure did not quite depend on the substrate characteristics, for example, hydrophilic or hydrophobic properties.

Thin Films of ca. 100 nm Thickness. Figures 3 and 4 show the AFM images of the PS/PMMA (50/50) and (30/70) thin films of 100 nm thicknesses coated on the gold substrate, respectively. The gold substrate was used in order to prepare the surface without any preferential adsorption of one component. In the case of the PS/PMMA (50/50) thin film, a well-defined sea-island-like phase-separated structure was observed at the film surface. The isolated domain height was about 20−40 nm, and the diameter of the domains was about 1−3 μm. Also, surface phase-separated structure with continuous-phase-like domains was observed in the case of the PS/PMMA (30/70) thin film. The continuous-phase-like domain height was about 20 nm. Since the domain area fraction increases with an increase in the PMMA bulk fraction, it seems reasonable to conclude that the domain region is composed of the PMMA phase. Figure 5 shows the AFM image of the PS/PMMA (30/70) thin film of 100 nm thickness coated on the gold substrate after the surface etching treatment with cyclohexane for 15 min, which is a good solvent only for PS segments. Also, Figure 5 shows the sectional view along the line shown in the AFM image. It is apparent from Figures 4 and 5 that the difference in height between PMMA domains and the PS matrix at the film surface drastically increases after the surface etching treatment with cyclohexane. Therefore, this result indicates again that the domains and the matrix regions are composed of the PMMA and the PS phases, respectively, as concluded from the variation of the domain−matrix area fraction. Also, Figures 4 and 5 exhibit that the PMMA continuous domains became more isolated after the surface etching treatment with cyclohexane. This indicates that the PMMA continuous domains are composed of the PMMA rich phase, in other words, slightly mixed with PS segments because the PMMA continuous domains are partially dissolved with a good solvent only for PS segments.

The air−polymer interface of the PS/PMMA thick film of 25 μm thickness prepared by a solvent-casting method was covered with a PS overlayer, as mentioned in Figure 1. On the other hand, in the case of the PS/PMMA thin film of 100 nm thickness coated by a spin-coating method, both PS and PMMA rich phases were observed at the air−polymer interface, as shown in Figure 4. The surface covered with PS segments with lower surface free energy is thermodynamically most stable. However, in the case of a spin-coating method, since solvent molecules are evaporated fairly fast from the solution before attainment of an equilibrium and thermodynamically stable state, the chain conformation or chain aggregation structure is generally frozen in the thin film before the formation of the most stable surface structure. Then, it seems reasonable to conclude that the discrepancy of surface structure between the thick film and the thin one may be attributed to the difference of the time required for the rearrangement for stable chain conformation.

Figure 6 schematically shows the formation process of the surface phase-separated structure during evaporation of solvent for the PS/PMMA thin film coated on

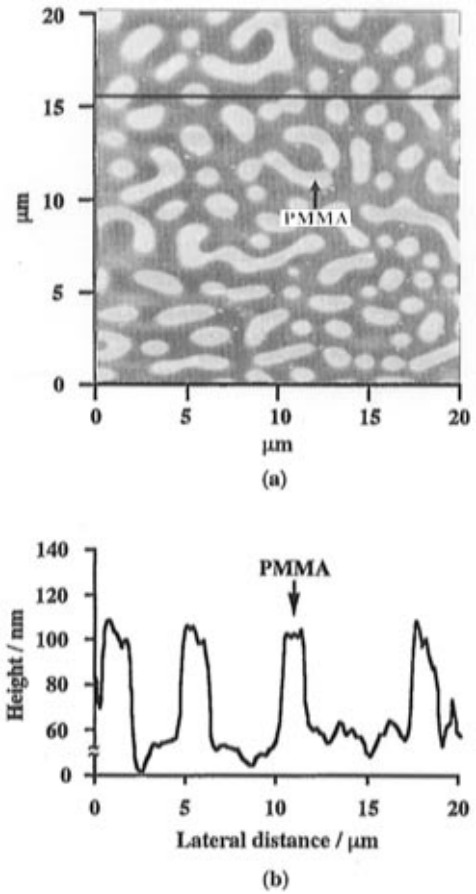

Figure 5. (a) AFM image and (b) sectional view along the line in the AFM image for the PS/PMMA (30/70) thin film of 100 nm thickness coated on the gold substrate after the surface etching treatment with cyclohexane.

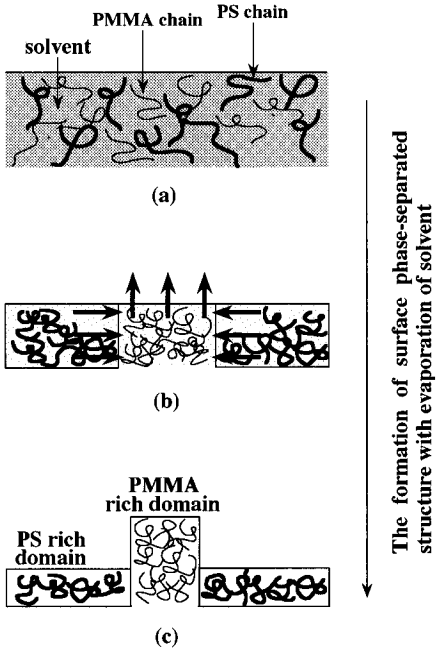

Figure 6. Schematic representation of the formation process of the surface phase-separated structure of the PS/PMMA thin film. (a) The top diagram shows PS and PMMA segments in a solution. (b) The center diagram corresponds to formation of the phase-separated structure on the way. (c) The bottom picture shows a completed phase-separated morphology.

the gold substrate. The surface area fraction of the PMMA rich phase was fairly smaller than that corresponding to the bulk PMMA weight fraction, and also, the PMMA rich domains finally separated out of the film surface, as shown in Figure 6c. The formation process of the surface phase-separated structure can be explained as follows. PS segments with lower surface free energy tend to cover the air−polymer interfacial region in order to minimize the interfacial free energy. However, in the case of the PS/PMMA thin film, since the time required for the surface structure is fairly short due to a very fast evaporation of solvent from the surface in comparison with that of the thick film, the surface structure composed of both PS and PMMA rich phases containing a little residual solvent is formed as shown in Figure 6b. At the stage of Figure 6b, although the large scale surface rearrangement cannot be attained, a local surface rearrangement of main chains can be fully attained in the thin film due to the presence of the residual solvent. Then, the PS rich phase is preferably spread out over the film surface. Therefore, if the total surface area of the thin film remains constant, the PMMA rich phase protrudes from the film surface, as shown in Figure 6c.

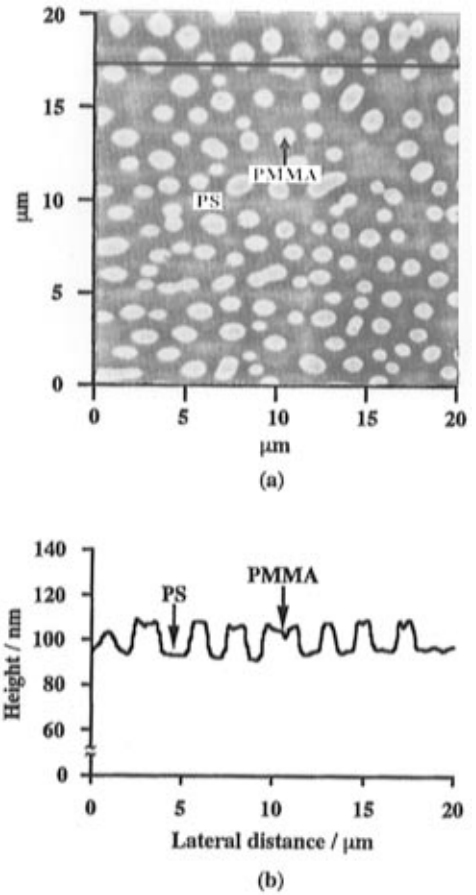

Figure 7. (a) AFM image and (b) sectional view along the line in the AFM image for the PS/PMMA (30/70) thin film of 100 nm thickness coated on the hydrophilic silicon substrate.

Next, the substrate dependence of the surface phase-separated structure for the thin film will be discussed. Figures 7 and 8 show the AFM images of the PS/PMMA (30/70) thin films coated on the hydrophilic silicon wafer and the hydrophobic siliconized cover glass, respectively, of which the thicknesses are 100 and 120 nm, respectively. It is apparent from Figures 4 and 7 that the PMMA domain size and shape are dependent on the kind of substrate, that is, gold and silicon wafer substrates. Since PMMA segments are preferentially adsorbed on the hydrophilic silicon substrate due to a

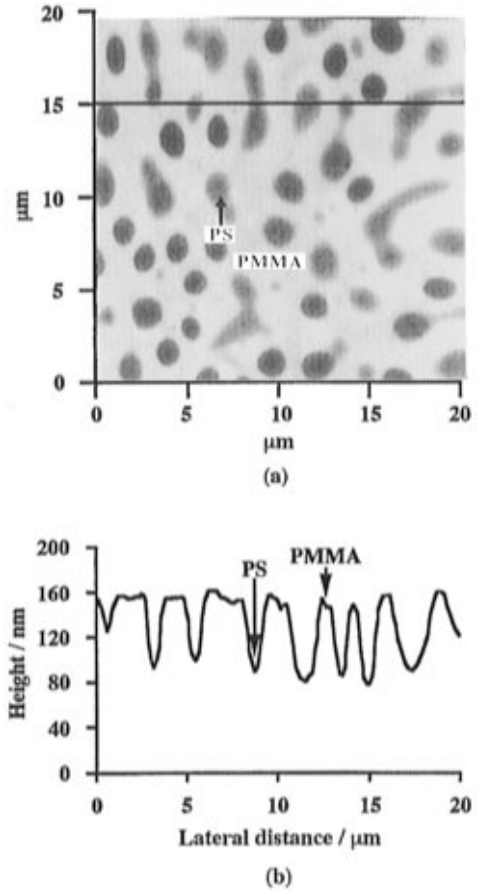

Figure 8. (a) AFM image and (b) sectional view along the line in AFM image for the PS/PMMA (30/70) thin film of 120 nm thickness coated on the hydrophobic siliconized cover glass.

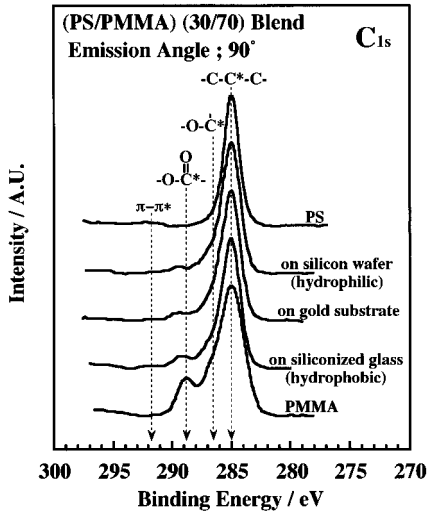

Figure 9. XPS C_{1s} core-level spectra of the PS/PMMA (30/70) thin films of 100 nm thickness coated on various substrates and of PS and PMMA homopolymers. All neutral C_{1s} peaks were assigned a binding energy of 285.0 eV to correct for the charging energy shift. The spectral intensities are normalized using the intensity for the PS/PMMA blend film.

Table 2. Substrate Effect on the Area Fraction of the PMMA Rich Phase and the PMMA Weight Fraction at the Surface for the PS/PMMA (30/70) Thin Films

substrate	water contact angle of substrate/deg	area fraction[a] of PMMA rich phase/%	PMMA weight fraction[b]/%
silicon wafer	0.0	23.9	16.8
gold		38.4	31.6
siliconized cover glass	88.7	66.7	52.8

[a] By AFM observation. [b] By XPS measurement.

fairly strong attractive interaction between the carbonyl groups of PMMA and the silanol groups on the silicon wafer[26] in comparison with the surface of the gold substrate, the PMMA weight fraction at the air–polymer interface must be decreased, as shown in Figure 7. The PMMA rich domain height and diameter for the PS/PMMA thin film coated on the silicon wafer were about 15–20 nm and ca. 1–2 μm, respectively. On the other hand, in the case of the PS/PMMA thin film coated on the siliconized cover glass as shown in Figure 8, the reverse sea-island-like phase-separated structure was observed on the film surface; that is, the bright and dark parts were reversed in comparison with Figure 7. The bright and the dark portions correspond to the continuous matrix and the isolated domain, respectively. On the basis of the experimental results on both the variation of the matrix area fraction with the PMMA bulk fraction and the change of the domain height after the surface treatment with cyclohexane, it can be concluded that the sea-like matrix in Figure 8 is composed of the PMMA rich phase; in other words, the isolated domains are composed of the PS rich phase. This result can be explained by the selective adsorption of PS segments with lower surface free energy to the hydrophobic siliconized glass substrate in order to minimize the polymer–substrate interfacial free energy. The substrate dependence on the surface structure of the PS/PMMA thin film was apparent, as shown in Figures 4, 7, and 8, and its effect was most remarkable, as the film thickness was about 100 nm.

XPS measurements were performed to evaluate the surface polymer composition of the blend thin films. Figure 9 shows the XPS C_{1s} spectra for the PS/PMMA (30/70) thin films of 100 nm thickness coated on various substrates and also the PS and the PMMA homopolymer films. Curve fitting of the C_{1s} spectra was achieved on the basis of a nonlinear least-squares method. A Gaussian function was assumed for each curve. The C_{1s} peak corresponding to neutral carbons was observed at 285.0 eV. The C_{1s} peaks observed at 286.5 and 288.8 eV were assigned to ether carbon and carbonyl carbon, respectively. Also, the C_{1s} shake-up peak corresponding to $\pi-\pi^*$ transition of the benzene ring was observed at 291.5–292.0 eV. The surface PMMA weight fraction, ω was calculated as follows. First, the C_{1s} spectra were separated into the four peaks corresponding to neutral, ether, and carbonyl carbon and shake-up of $\pi-\pi^*$ transition of the aromatic group. Then, ω values were calculated by using eq 2,

$$\frac{I_{C=O} + I_{C-O}}{I_{total}} = \frac{2\omega/M_{MMA}}{\frac{8(1-\omega)}{M_S} + \frac{5\omega}{M_{MMA}}} \qquad (2)$$

where I_i is the integrated intensity of a core-electron photoemission spectrum. M_S and M_{MMA} are the molecular weights for styrene and methyl methacrylate monomer units, respectively.

Table 2 shows the substrate effect on the surface area fraction of the PMMA rich phase and the surface PMMA weight fraction for the PS/PMMA (30/70) thin film of about 100 nm thickness. Each magnitude was evaluated on the basis of AFM observation and XPS mea-

surement, respectively. The surface area fraction of the PMMA rich phase and the surface PMMA weight fraction increased with an increase in water contact angle of the substrate, that is, a decrease in surface free energy of the substrate. Also, the magnitude of the surface area fraction of PMMA rich phase is larger than that of the surface PMMA weight fraction for all the specimens. In general, in the case of the A/B binary polymer blends, one phase of the phase-separated structure is the component A rich phase and the other is the component B rich phase. The rich phase means that one component contains or dissolves a small amount of the other component. Since the PMMA rich phase contains a small amount of PS segments, the PS chains in the PMMA rich domains are enriched at the air−polymer interface in order to minimize the air−polymer interfacial free energy. Thus, it seems reasonable that the magnitude of the surface area fraction of the PMMA rich phase is higher than that of the surface PMMA weight fraction.

Two-Dimensional Ultrathin Films of 10.2 and 6.7 nm Thicknesses. The polymeric blend films with thicknesses less than $2R_g$ of the higher molecular weight component can be defined as the two-dimensional ultrathin blend films.[20] Figure 10 shows the AFM image of the two-dimensional PS/PMMA (30/70) ultrathin film of 10.2 nm thickness coated on the gold substrate. Distinct surface phase-separated structure was not observed in this image. However, a little variation of contrast on the surface was recognized as the image was magnified. In the case of an individual chain in a constrained two-dimensional ultrathin state, its conformational entropy is reduced in comparison with that in a three-dimensional solid state.[19] This means that the number of pair interaction between foreign segments in the two-dimensional ultrathin blend film is reduced in comparison with that in a three-dimensional solid state. Since the interaction between PS and PMMA segments is the repulsive, Flory−Huggins interaction parameter, χ_{2d} is smaller than χ_{3d} where the subscript 2d or 3d denotes the dimension in the film and, then, the miscibility in the two-dimensional ultrathin film might be improved. Thus, it seems quite reasonable that distinct surface phase-separated structure is not observed for the PS/PMMA ultrathin film of 10.2 nm thickness, as shown in Figure 10. Also, it was apparent that the surface structure for the ultrathin film did not depend on the substrate characteristics due to difficulty in enrichment of the one component to the substrate in the case of the ultrathin layer with the thickness less than $2R_g$.

Figure 11 shows the AFM topographic image of the two-dimensional PS/PMMA (30/70) ultrathin film of 6.7 nm thickness coated on the gold substrate. When the film thickness became thinner than 10.2 nm, a fine and distinct surface phase-separated structure appeared again, as shown in Figure 11. The domain height was about 3 nm. In order to confirm if the surface structure such as Figure 11 was attributed to the dewetting of polymer chains on the substrate, XPS measurement was performed. Since the magnitude of the ratio of the XPS peak intensities for Au_{4f} to C_{1s} was very small compared with that assuming the dewetting structure in which the dark part in Figure 11 was composed of the bare Au substrate, it was apparent that the photoelectrons emitted from Au atoms decreased with polymer overlayer on the substrate; that is, the substrate was almost completely covered with polymer chains.

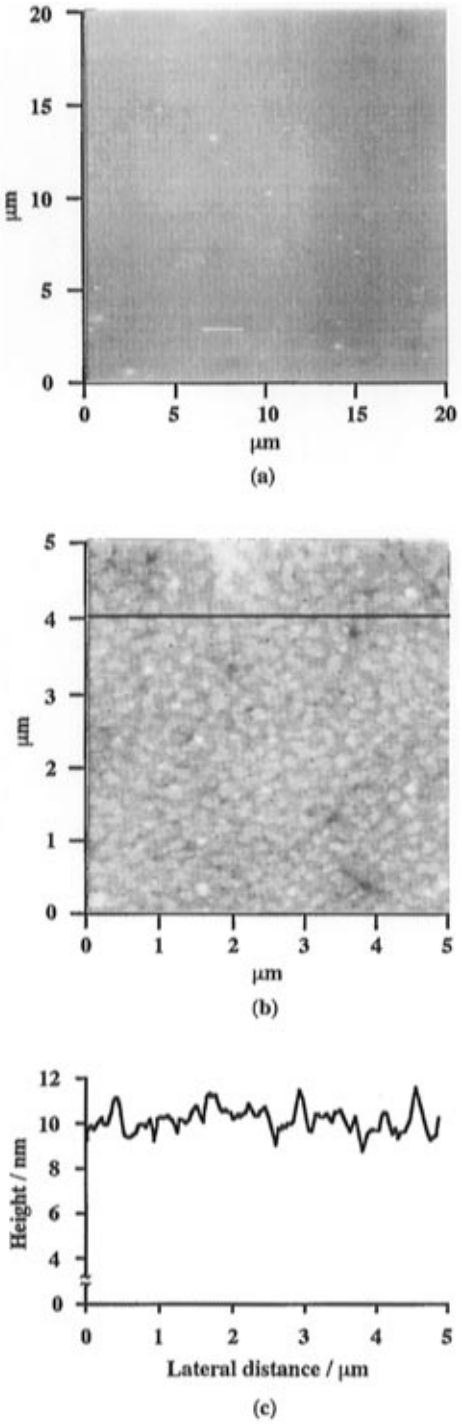

Figure 10. (a) AFM image and (b) enlarged image of the partial area of (a) for the two-dimensional PS/PMMA (30/70) ultrathin film of 10.2 nm thickness coated on the gold substrate. (c) Sectional view along the line in the topographic image (b).

As mentioned above, the phase-separated structure with a domain size of a few hundred nanometers was observed at the ultrathin film surface, as shown in Figure 11. This aggregation structure can be designated as "mesoscopic phase-separated structure". AFM observation and XPS measurement revealed that the surface matrix area fraction and the surface PMMA weight fraction were about 70%, corresponding to the PMMA bulk weight fraction. Since molecular chains are almost isolated in the extremely constrained two-dimensional state,[27] it is reasonable to consider that the PMMA weight fraction is constant along the thick-

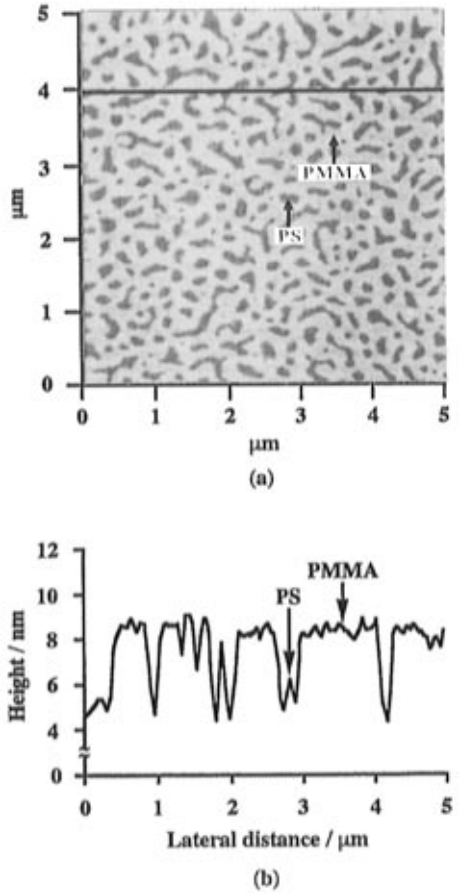

Figure 11. (a) AFM image and (b) sectional view along the line in the AFM image for the PS/PMMA (30/70) ultrathin film of 6.7 nm thickness coated on the gold substrate.

ness direction. Thus, it seems reasonable to conclude that the bright matrix portion of Figure 11 is composed of the PMMA component.

As discussed in the previous section, in the case of the two-dimensional PS/PMMA ultrathin film, the miscibility of PS segments to PMMA ones increases with a decrease in the film thickness, because χ_{2d} decreases with a decrease in the film thickness. However, this prediction was opposite to the result of AFM observation for the ultrathin blend film of 6.7 nm thickness, as shown in Figures 10 and 11. In the two-dimensional ultrathin blend film, the miscibility is fairly affected by two factors: the decrease in the conformational entropy and the appearance of the individual character of a molecular chain. The decrease in χ_{2d} induced by the decrease in the conformational entropy makes the miscibility of the blend system increase. On the other hand, when the character of a molecular chain appears, that is, a molecular chain is isolated, the blend system is in a phase-separated state and this effect becomes more remarkable as the film thickness becomes thinner. Shuto et al. investigated the aggregation state of a molecular chain in the two-dimensional ultrathin film on the basis of small angle X-ray and neutron scattering measurements.[18] They concluded that, when the magnitude of two-dimensionality, D, which was given by the ratio of the film thickness to $2R_g$, was less than 0.5, the degree of interpenetration by the surrounding chains decreased and, then, the entanglement among polymer chains decreased.[18] Also, de Gennes expected that polymer chains in the extremely constrained two-dimensional state were almost isolated along the perpendicular direction to the film surface and stretched along the parallel direction with a little interpenetration by the surrounding chains.[27] Thus, in the case of the two-dimensional ultrathin blend film of 6.7 nm thickness ($D = 0.40$), molecular chains are almost isolated along the thickness direction and, then, the character of a molecular chain directly appears at the surface in the extremely constrained two-dimensional state. Therefore, in the case of the two-dimensional PS/PMMA ultrathin film of 6.7 nm thickness, it seems reasonable to conclude that fine and distinct surface phase-separated structure appears again, as shown in Figure 11.

Conclusions

It has been shown that the surface structure of the PS/PMMA blends depends on the film thickness. As in the case of the PS/PMMA blend film of 25 μm thickness, the air−polymer interfacial region was covered with a PS rich overlayer due to its lower surface free energy compared with that of PMMA and well-defined macroscopic phase-separated structure was formed in a bulk phase. The surface structure of the PS/PMMA thick film did not depend on the magnitude of surface free energy of the substrate. Also, in the case of the PS/PMMA thin film of 100 nm thickness coated on the gold substrate, the phase-separated structure, in which PMMA rich domains separated out of the PS rich matrix, formed at the film surface. The formation of the surface structure for the PS/PMMA thin film could be attributed to either the chain conformation or chain aggregation structure being frozen at the air−polymer interfacial region before the formation of a PS rich overlayer due to the fairly fast evaporation of solvent molecules. Both the area fraction of the PMMA rich phase and the PMMA weight fraction at the air−polymer interface for the PS/PMMA thin film of 100 nm thickness were fairly dependent on the magnitude of surface free energy of the substrate. The substrate dependence of the surface structure for the PS/PMMA film became most remarkable when the film thickness was about 100 nm. On the other hand, the two-dimensional PS/PMMA ultrathin film of 10.2 nm thickness did not show distinct surface phase-separated structure, which did not depend on the substrate characteristics. When the film thickness became thinner, as in the case of the two-dimensional PS/PMMA ultrathin film of 6.7 nm thickness, a fine and distinct phase-separated structure with a domain size of a few hundred nanometers, which could be designated as "mesoscopic phase-separated structure", was observed at the film surface again. The surface phase state for the two-dimensional PS/PMMA ultrathin films can be explained by the film thickness dependence of both the Flory−Huggins interaction parameter and the degree of entanglement among polymer chains.

Acknowledgment. This work was partially supported by Research Fellowships of the Japan Society for the Promotion of Science for Young Scientists.

References and Notes

(1) Hasegawa, H.; Hashimoto, T. *Macromolecules* **1985**, *18*, 589.
(2) Bhatia, Q. S.; Pan, D. H.-K.; Koberstein, J. T. *Macromolecules* **1988**, *21*, 2166.
(3) Green, P. F.; Christensen, T. M.; Russell, T. P.; Jerome, R. *Macromolecules* **1989**, *22*, 2189.
(4) Takahara, A.; Jo, N.-J.; Kajiyama, T. *J. Biomater. Sci., Polym. Ed.* **1989**, *1*, 29.

(5) Teraya, T.; Takahara, A.; Kajiyama, T. *Polymer* **1990**, *31*, 1149.
(6) Takahara, A.; Korehisa, K.; Takahashi, K.; Kajiyama, T. *Kobunshi Ronbunshu* **1992**, *49*, 275.
(7) Cowie, J. M. G.; Devlin, B. G.; Mcwen, I. *Polymer* **1993**, *34*, 501.
(8) Mori, H.; Hirao, A.; Nakahama, S.; Senshu, K. *Macromolecules* **1994**, *27*, 4093.
(9) Jones, R. A. L.; Kramer, E. J. *Polymer* **1993**, *34*, 115.
(10) Meyers, G. F.; DeKoven, B. M.; Seitz, J. T. *Langmuir* **1992**, *8*, 2330.
(11) Mayes, A. M. *Macromolecules* **1994**, *27*, 3114.
(12) Kajiyama, T.; Tanaka, K.; Ohki, I.; Ge, S.-R.; Yoon, J.-S.; Takahara, A. *Macromolecules* **1994**, *27*, 7932.
(13) Kajiyama, T.; Tanaka, K.; Takahara, A. *Macromolecules* **1995**, *28*, 3482.
(14) Tanaka, K.; Takahara, A.; Kajiyama, T. *Acta Polym*. **1995**, *46*, 476.
(15) Keddie, J. L.; Jones, R. A. L.; Cory, R. A. *Europhys. Lett*. **1993**, *23*, 579.
(16) Reiter, G. *Macromolecules* **1994**, *27*, 3046.
(17) Shuto, K.; Oishi, Y.; Kajiyama, T.; Han, C. C. *Polym. J*. **1993**, *25*, 291.
(18) Shuto, K.; Oishi, Y.; Kajiyama, T.; Han, C. C. *Macromolecules* **1993**, *26*, 6589.
(19) Shuto, K.; Oishi, Y.; Kajiyama, T. *Polymer* **1995**, *36*, 549.
(20) Tanaka, K.; Yoon, J.-S.; Takahara, A.; Kajiyama, T. *Macromolecules* **1995**, *28*, 934.
(21) Shiraga, N.; Tanaka, K.; Minobe, M. *Kobunshi Ronbunshu* **1992**, *49*, 353.
(22) Riemann, R.-E.; Braun, H.; Weese, J.; Schneider, H. A. *New Polym. Mater*. **1994**, *4*, 131.
(23) Li, L.; Sosnowski, S.; Chaffey, C. E.; Balke, S. T.; Winnik, M. A. *Langmuir* **1994**, *10*, 2495.
(24) Ballard, D. G. H.; Wignall, G. D.; Schelten, J. *Eur. Polym. J*. **1973**, *9*, 965.
(25) Owens, D. K.; Wendt, R. C. *J. Appl. Polym. Sci*. **1969**, *13*, 1741.
(26) Mayes, A. M.; Russell, T. P.; Baker, S. M.; Smith, G. S. *Macromolecules* **1994**, *27*, 749.
(27) de Gennes, P.-G. *Scaling Concepts in Polymer Physics*; Cornell University Press: Ithaca, NY, 1979.

MA951140+